NIH Public Access
Author Manuscript
Small. Author manuscript; available in PMC 2010 April 23.

Published in final edited form as:
Small. 2010 April 23; 6(8): 937–944. doi:10.1002/smll.200902326.

Interface Directed Self Assembly of Cell-Laden Microgels

Behnam Zamanian[*,1,2], **Mahdokht Masaeli**[*,1,2,3], **Jason W. Nichol**[1,2], **Masoud Khabiry**[1,2], **Matthew J. Hancock**[1,2], **Hojae Bae**[1,2], and **Ali Khademhosseini**[1,2,†]

[1] Center for Biomedical Engineering, Department of Medicine, Brigham and Women's Hospital, Harvard Medical School, 65 Landsdowne Street, Cambridge, MA 02139, USA

[2] Harvard-MIT Division of Health Sciences and Technology, Massachusetts Institute of Technology, Cambridge, MA 02139, USA

[3] Department of Electrical and Computer Engineering, Northeastern University, Boston, MA 02115, USA

Abstract

Cell-laden hydrogels show great promise for creating engineered tissues. However, a major shortcoming with these systems has been the inability to fabricate structures with controlled microscale features on a biologically relevant length scale. Here we demonstrate a rapid method for creating centimeter-scale, cell-laden hydrogels through the assembly of shape-controlled microgels. This was achieved by using an approach that uses the liquid-air interface of a hydrophobic solution to drive the assembly of microgels. Cell-laden microgels of specific shapes were randomly placed on the surface of a high density, hydrophobic solution and induced to aggregate and were subsequently crosslinked into macroscale tissue-like structures. The resultant assemblies were cell-laden hydrogel sheets consisting of tightly-packed ordered microgel units. In addition, a hierarchical approach created complex multi-gel building blocks which were then assembled into tissues with precise spatial control over the cell distribution. These data demonstrate that forces at an air-liquid interface can be used to self-assemble spatially controllable, co-cultured tissue-like structures.

Keywords

self assembly; microgel; bottom-up; tissue engineering

Introduction

Organ failure is one of the major causes of death worldwide. [1] However, the number of people who need organ transplants is significantly higher than the number of available organs suitable for transplantation.[1] As a result, fabrication of three dimensional (3D) organs is of great importance for regenerative medicine.[2] Recent results have demonstrated the importance of tissue microarchitecture on the resulting function of engineered tissue constructs,[3] therefore devising more biomimetic techniques for generating engineered tissues with microscale resolution is of great scientific interest.

† Corresponding author: Ali Khademhosseini, PhD (alik@rics.bwh.harvard.edu) Partners Research Building, Rm 252, 65 Landsdowne Street Cambridge MA, USA 02139 Fax: (617) 768-8395.
*The authors contributed equally to this work.

Author contributions: BZ, MM and AK conceived of the project, designed methodology and the experiments, BZ, MM and HB performed the experiments and the immunostaining, BZ, MM and MK analyzed the data. BZ, MM, JN, and AK wrote the manuscript; MJH wrote the theoretical rationale. All authors revised the manuscript and consented to the contents of the final version.

NIH-PA Author Manuscript
NIH-PA Author Manuscript
NIH-PA Author Manuscript

NIH-PA Author Manuscript

NIH-PA Author Manuscript

NIH-PA Author Manuscript

Microfabrication technologies have been applied to cell culture techniques in an effort to better direct tissue formation and function.[4] As cell-cell and cell-extracellular matrix (ECM) interactions play critical roles in cell and tissue function, control over the cellular microenvironment could be key to fabricating biomimetic tissue structures.[4] The tissue microarchitecture in the human body is often made of repeating functional units, such as the repeating hexagonal lobules in the liver. [5] As a result, self assembly of microscale tissues that can recreate the native microarchitecture of natural tissues, could be a promising approach for fabrication of functional tissue constructs.

Self assembly at various length scales has been previously used for creating complex structures. [6, 7] For example, self assembly has been used at the molecular scale to synthesize biomaterials, and at the mesoscale to generate structures both in two dimensional (2D) arrays, and 3D mesostructures. Cellular assembly has also been used to create complex tissue structures such as rods, tori, honeycombs,[8, 9] knee cartilage,[10] and capillary filtration devices.[11] We have previously demonstrated the self assembly of cell-laden microgels by immersion of hydrophilic cell-laden hydrogels into hydrophobic solutions.[7] Higher order structures were created in predictable patterns and dimensions through control over hydrophilic microgel aggregation and subsequent secondary polymerization. We also demonstrated that through the specific design of microgel dimensions and geometry, i.e. lock- and-key shapes, gels could be directed to create ordered co-cultured constructs. Overall, many positive characteristics and features of self assembly techniques have been demonstrated, however major limitations still exist regarding the achievable sizes, shapes and organization of the resulting fabricated structures.

The encapsulation of cells within cell-laden microgels is an attractive approach for engineered tissue formation.[12, 13] In particular, microgels provide control over the cell-cell and cell-ECM contacts found within the cellular microenvironment that can be used to improve the resulting cellular organization and function.[14] Furthermore, since each microgel can be fabricated with unique properties, it is possible to engineer tissues with multiple chemical microenvironments. In addition, encapsulation of different growth factors, drugs or other deliverable molecules in separate blocks is achievable.[14] Employing photolithography techniques enables the engineering of building blocks with tunable microarchitectures to better control the cellular microenvironment, while self assembly techniques have demonstrated the ability to somewhat control the macroscale environment of the resulting engineered tissues.[7]

Here we describe a technique for self assembly of cell-laden microgels on the interface of air and hydrophobic solutions to fabricate 3D tissue constructs with controllable microscale features. This self assembly process is guided by the surface tension forces at the liquid-air interface[6, 15] of high density, hydrophobic solutions. The hight density solution forced the lower density hydrophilic hydrogels to remain on the surface similar to techniques previously reported for inorganic materials.[6, 16] Hydrophilic, cell-laden hydrogels were randomly placed on the surface of high density, hydrophobic solutions. Surface tension drove the microgels toward each other to create tissue-like structures through aggregation.[15] These basic thermodynamic mechanisms enabled the fabrication of centimeter scale tissue structures from cell-laden microscale hydrogels. The ability to create tissues with these length scales and a clinically relevant overall size suggests that this technique may be beneficial for tissue engineering applications.

Results and Discussion

In this study we fabricated centimeter scale tissues from microgel building blocks by using a directed self assembly approach that utilizes the air-liquid interface. We also demonstrated

NIH-PA Author Manuscript

NIH-PA Author Manuscript

NIH-PA Author Manuscript

that a modified version of this process can be used to create centimeter scale tissues with spatially controlled 3D co-cultures. The resultant tissue constructs have microscale features combined with clinically relevant length scales suggesting potential use for tissue repair and regeneration.

Self assembly process

PEG hydrogel building blocks of specified geometry and dimensions were created as described (Figure 1, A-C) and randomly placed on the surface of carbon tetrachloride (CCl_4) or perfluorodecalin (PFDC) (Figure 1, D) to fabricate three-dimensional (3D) tissue-like constructs. From a list of potential solutions, PFDC and CCl_4 were chosen because they were denser than water, ensuring the microgel blocks would float, and because of their hydrophobicity, which kept the hydrogel blocks on the surface and helped induce aggregation.[6, 16] However only PFDC was used in cell-laden assembly experiments, due to the excessive toxicity caused by CCl_4 exposure.[17] Due to the surface tension on the liquid-air interface, the hydrogels moved towards each other and began aggregating to minimize the system free energy (Figure 1, E). Since the hydrogels were bound only through minimization of the surface free energy, a secondary crosslinking step was used to stabilize the microgel assemblies and create centimeter-scale tissue structures (Figure 1, F). No additional unreacted PEG is necessary to add to be able to achieve secondary and tertiary polymerizations, consistent with previous studies.[7] This technique, which exposed the gel blocks to ultraviolet (UV) light for a short time, successfully formed tightly packed, centimeter scale 3D tissue sheets consisting of multiple microgel subunits with square, triangle and hexagonal geometries (Figure 2). While this technique could be used with a wide variety of microgel shapes, the optimum microgel geometry for cell and tissue function may not always correlate with optimum aggregation. The resulting cell sheets could be potentially used for tissue engineering applications of vascular,[18] corneal, bladder and other tissues with the added benefit of controlling the cellular microenvironment in 3D.

Previously, self assembly has shown great potential, yet with inherent limitations for various applications such as tissue engineering. For example, Whitesides and colleagues developed approaches to assemble mesoscale structures with similar conceptual elements to the present work.[6, 16] Their work demonstrated the utility of self assembly of polydimethylsiloxane (PDMS) modules on the surface of PFDC. Improved control over the assembly process was implemented by rendering certain faces of the modules hydrophobic or hydrophilic. However, PDMS modules were unable to bind following aggregation, limiting their utility when not on the solution surface and making removal of the assembled structures difficult. In contrast, by using hydrogels, our system was able to use cell-laden modules for creating engineered tissues. In a previous report, we demonstrated the self assembly of cell-laden PEG microgels within hydrophobic mineral oil to create higher order structures.[7] Drawbacks of the previous technique include the limited control over the resulting sizes of the assembled structures, which were in the microscale range, as well as limitations on the efficiency of the assembly process. Assembling cell-laden microgels on a dense hydrophobic surface allows for much greater overall structure sizes, in the centimeter scale. The corrent technique also offers greater control on the directed assembly process, at micro and macro dimensions, than previous techniques which employed random assembly only within defined containment structures, such as perfusion tubing,[19] or cells seeded onto structures following creation.[8, 9]

Cell viability

To assest the effects of UV exposure and the assembly process on cell viability, samples were collected following each step of the procedure and analyzed using a live/dead assay (Figure 3). Cell viability was determined for cells mixed in the prepolymer solution,

NIH-PA Author Manuscript

NIH-PA Author Manuscript

NIH-PA Author Manuscript

following the 27 second UV exposure leading to polymerized microgels (Figure 3, A-B), after 1 min exposure of cell-laden microgels to the surface of PFDC (Figure 3, C), and following secondary UV exposure for 5 seconds leading to 3D tissue formation in PFDC (Figure 3, D). Cell-laden microgels were then cultured statically in basal media with viability determined on days 1, 3, 5 and 7 (Figure 3, E-H), while quantification of viability was performed for 5 samples for each condition (Figure 3, I). The live/dead analysis demonstrates that viability remained above 90% following UV and PFDC exposure, demonstrating that neither significantly affected cell viability. In summary, throughout the fabrication and assembly processes, cell viability remained virtually unchanged. Cell viability was then tracked over a 1-week period to assess the feasibility of the current assembly technique for creating long-term engineered tissues. Viability remained above 90% on days 1 and 3, and still remained at or above 85% up to 1 week. There were no significant losses in viability throughout the process or subsequent culture, demonstrating the suitability of this technique for creating robust long-term tissue-like structures. As UV and PFDC exposure has been demonstrated to show no significant effect on short term or long term cell viability, we believe this strongly suggests that binding multiple microgel sheets together to form 3D tissue structures would not be prevented by potential cell viability loss due to excessive UV exposure. In addition, provided the exposure times remain on the order presented, increasing the number of UV and PFDC exposures to create more intricate microgel assemblies should not significantly alter either the short or long term viability in assembled structures.

Theoretical rationale

Solid particles floating on the surface of a dense liquid can deform the liquid surface thereby generating lateral capillary forces which may be repulsive or attractive depending on the particle weight, geometry and wetting properties.[20-22] The capillary forces move the floating particles so as to reduce the total free surface area and the system energy. By tuning the mass and the geometrical and wetting properties, the particles can self assemble into various patterns.[6, 23, 24] In general, it has been found experimentally and theoretically that particles aggregate based on the simple rule “like menisci attract, and unlike menisci repel”. Since our system is composed of identical particles, these will attract. The degree of attraction and hence the speed of aggregation depends on the wetting and geometrical properties of the particular solid particle-liquid combination. The capillary forces extend over a length scale $l_c = \sqrt{\gamma/\rho g}$, the capillary length, where γ is the surface tension of the gas/fluid interface, ρ is the fluid density, and g is the acceleration of gravity. For CCl_4 at 25°C,[25, 26] ρ = 1.58 g mL^{-1}, γ = 26.1 dynes cm^{-1} and l_c = 1.3 mm; for PFDC,[27, 28] ρ = 1.93 g mL^{-1}, γ = 19.4 dynes cm^{-1} and l_c = 1.0 mm. The relative importance of gravity and surface tension is quantified by the (dimensionless) Bond number, $B_0 = (d/l_c)^2$, where d is the particle diameter. In our system, d = 200 – 1000 μm and B_0 = 0.024 – 0.60 for CCl_4 and B_0 = 0.039 – 0.98 for PFDC. Hence for the smaller sizes capillary forces dominate gravity and particles rely primarily on their geometry and wetting properties, and not their weight, to deform the free surface and experience the concomitant capillary forces. Capillary attraction between light particles dominates thermal energy for particle sizes down to the nanometer scale.[15, 29] Lastly, since viscous drag on a particle scales as its surface area and the capillary force as its diameter, drag becomes less important as particle sizes are reduced. Thus the capillary force driven self assembly observed in our model system is scalable to the nanometer scale.

Theoretical approaches could be used to tune the particle design and wetting properties to optimize the self assembly process in our system. The static free surface is described by the Young-Laplace equation, which admits analytic solutions for simple geometries such as the free surface between parallel infinite walls or cylinders.[30, 31] For more complex geometries like spherical, square, triangular, and hexagonal bodies, the free surface must be computed

NIH-PA Author Manuscript

NIH-PA Author Manuscript

NIH-PA Author Manuscript

numerically, though approximate formulas exist for small surface slopes and large particle spacing.[15, 20, 32-35]

Aggregation factor and parameter optimization

To fabricate tissue-like constructs with physiologically relevant cell densities, geometries and microarchitecture, it is essential to maximize the microgel packing by optimizing the microgel aggregation. To achieve this goal several parameters were optimized, such as the molecular weight of PEG, microgel dimensions, and the number of microgels in the hydrophobic solution. To evaluate the parameter optimization, an aggregation factor (A_f) was defined as follows:

$$A_f = 1 - \frac{a_f}{n \times a_i} \quad (1)$$

where a_f is the sum of the areas of the microgel faces in contact with the interface (i.e. the contact line), a_i is the sum of the areas of the faces of one microgel in contact with the interface, and n is the total number of microgels. In the case where there is no aggregation $a_f/(na_i) = 1$ and $A_f = 0$. Figure 4 A-D illustrates the gradual increase of the aggregation factor as the microgels aggregate. The red line shows the contact line where the interface meets the aggregated structure. Once microgels join the aggregated structure, a_f decreases and since a_i is constant for a specific microgel block, the aggregation factor A_f rises.

The evolution of the aggregation factor is shown in Figure 4 and demonstrates that the aggregation factor increased with time and PEG molecular weight. As time passed, surface tension had more time to aggregate the microgel blocks. Increasing the molecular weight of PEG improved aggregation by increasing the hydrophilicity of the microgels, thereby increasing the difference in initial and final free energy of the system (Figure 4A-D). Increasing the molecular weight of PEG from 258 to 4000 resulted in roughly a 3-fold increase in the aggregation factor from 12% to 35% (Figure 4E, $p < 0.05$). Similarly, increasing the thickness of the microgels from 300μm to 600μm more than tripled the aggregation factor from 10% to 33% (Figure 4F, $p < 0.05$). Also, increasing the number of initial building blocks from 20 to 50 increased the aggregation factor from 26% to 36% (Figure 4G, $p < 0.05$).

Effects of agitation on aggregation

To increase the packing density of the resulting macrostructures and to increase the speed and completeness of aggregation, centripetal forces were applied to the system by means of stirring. Stirring improves the aggregation by creating a depression on the free surface which allowed gravity to help drive the particles toward each other. We investigated two hydrophobic solutions, PFDC and CCl_4, each with four different rotational speeds (Figure 5). Stirring at a rate of 200 RPM increased the aggregation factor from 34% (no stirring) to 80% for CCl_4 ($p < 0.001$). Similar behavior was observed for PFDC when the rotational speed was increased from 0 RPM to 200 RPM, increasing A_f from 24% to 82%, respectively ($p < 0.001$). Furthermore, increasing the stirring speed to 300RPM significantly decreased the aggregation factor from 80% to 36% for CCl_4 and 82% to 36% for PFDC ($p < 0.001$). The optimized stirring speeds determined here depended on the solution volume and depth, and are therefore only valid for the conditions described.

While larger aggregate sizes were not attempted in this study, there should not be any physical limit to the overall structure size achievable using this technique. Given the availability of dishes with sufficiently large diameters, sufficient quantity of PFDC and a

NIH-PA Author Manuscript

NIH-PA Author Manuscript

NIH-PA Author Manuscript

large coverage area for the UV exposure (or multiple exposures covering smaller individual areas) any desired size seemingly could be constructed. In addition, while the overall structure shape tended to be circular, asymmetric shaped dishes, such as square or rectangular, could allow for more control over the shape of the assembly. However, this would likely also descrease the efficiency of aggregation as the stirring would not be applied equally to all regions. Another method for producing shaped assemblies whould be to creat cercular sheets and cutting them to shape. Though not optimally efficient, this method could rapidly produce controlled structure sizes and shapes since 10s to 100s of microgels can be created with 1 UV step and aggregated into sheets in minutes.

Spatial control of cell seeding in engineered tissue constructs

Fabricating complex tissues requires the co-culture of different cell types in physiologically relevant geometrical patterns. However, a limitation of many fabrication techniques is the lack of spatial control of specific cell types within engineered tissues. In this report, multiple cell-laden microgels of identical shape and dimensions were rapidly aggregated and polymerized into robust, 3D tissue-like constructs. While this approach facilitated rapid formation of tissue constructs, the microgel assembly was governed primarily by random interactions. Therefore, this technique could be used to create tissue layers with microgels of multiple cell types, but could not spatially control the co-cultured cell-laden microgels. To address this issue a hierarchical approach was investigated to facilitate spatial control over cell placement in the engineered tissues.

In the hierarchical approach, the tissue of interest is constructed through a multi-step process. Individual microgels of similar shape, each containing 1 cell type, were created as described previously, using either rhodamine or fluorescein isothiocyanate (FITC) labeled cells. Next, one hydrogel with rhodamine labeled cells was placed on the hydrophobic solution surface loosely surrounded by six hydrogels of the same structure with FITC labeled cells. The FITC-labeled microgels aggregated to form a fully packed structure surrounding the rhodamine labeled microgel. These fabricated structures were photocrosslinked and then used as building blocks for a subsequent assembly process to create centimeter scale, tightly packed tissues with spatially controlled co-culture. Figure 6A shows a cartoon representation of this process. Figures 6B and 6C show the phase contrast and fluorescent images of the consequent structure respectively. To enact even further control over co-culture and overall assembly parameters, lock and key structures were employed, furthere demonstrating the versatility of this technique (Figure 6, D-F).

While the creation of these complex, co-culture building blocks was more time consuming than with singular microgel building blocks, the hierarchical technique allowed for precise control over the co-culture cell distribution, while being compatible with the high throughput production of larg tissue-like sheets. Moreover, each complex building block was created in under 1 minute. These complex blocks could be produced in parallel and then rapidly assembled using a high throughput approach, making the overall technique still relatively rapid. One negative aspect of this multi-step approach was a reduced yield in complex building blocks which was balanced by the improved level of spatial control of cell deposition within the tissue-like constructs. The hierarchical technique combines many of the positive spatial cell seeding aspects of previous techniques like sequential photopolymerization or organ printing,[36, 37] but without the need for specialized equipment or technical expertise greatly increasing the possible applications and potential users.

In addition, we incorporated cell-responsive photocrosslinkable hydrogels with our assembly technique. Using gelatin methacrylate (GelMA), we demonstrated that co-cultured cells could migrate across microgel borders to interact with neighboring cells (Figure 6, G-H). The migration could be more precisely controlled through the creation of very specific

NIH-PA Author Manuscript

NIH-PA Author Manuscript

NIH-PA Author Manuscript

cell binding and degradation sites using PEG as described previously. [38, 39] One potential drawback to the presented technique is the necessity that any desired hydrogel must be polymerized through photocrosslinking, limiting the pool of available materials. However, as the data demonstrate, diminished viability due to UV exposure is not a major concern. In addition, UV crosslinking rapidly polymerizes the microgels (in seconds), avoiding the gravitational settling of cells and ensuring even cell distribution in 3D. Other polymerization techniques are not as rapid.

Conclusions

This work introduces a fabrication method for creating cell-laden tissue-like structures using a bottom-up self assembly approach in a multi-phase environment (liquid-air system). This technique can be used to rapidly create tightly packed tissue-like sheets with either single cell types or homogeneously distributed co-culture. In addition, a hierarchical approach was demonstrated which can create complex multi-gel building blocks with precisely controlled co-culture distribution to create tissue-like constructs with specific cell distribution. Even greater control over this technique can be achieved by using specific structures, such as lock and key assemblies, to better direct the assembly of co-cultured tissues. The ability to precisely control the cell distribution within self assembled tissue-like constructs could greatly improve engineered tissue function and morphology. This technique could create single layer implants, or could be combined with existing cell sheet techniques to create multilayer engineered tissues providing more control than is currently possible with traditional cell sheet techniques. Future works will expand the directed assembly technique to include more than two cell types, multiple shapes and more intricate lock and key assemblies, enabling advances in the field of engineered tissues with controlled cell distribution and microarchitectural features.

Experimental Section

Preparation of microgels

Microgels were prepared by dissolving 20% (w/w) poly(ethylene glycol) dimethacrylate (PEG, 4000 Da, Monomer-Polymer & Dajac Labs Inc.) in Dulbecco's phosphate buffered saline (DPBS; GIBCO). The hydrogel units were fabricated through UV polymerization on the surface of glass slides. To ease the detachment of the hydrogel from the glass surface following polymerization, glass slides were treated with ocadecyltrichlorosilane (OTS, Sigma) as previously described [7]. Before UV polymerization, 1% (w/w) photoinitiator 2-hydroxy-1-(4(hydroxyethoxy) phenyl)-2methyl-1propanone (Irgacure 2959; CIBA Chemicals) was added to the prepolymer solution. Photomasks, with different patterns and sizes (dimensions in μm; 200×200, 400×400, 600×600, 800×800, and 1,000×1,000) were designed in AutoCAD and printed on 20,000-dpi resolution transparencies (CAD/Art Services). Different basic shapes (square, triangular and hexagonal) were used to demonstrate the assembly technique's versatility and its utility to recreate a wide variety of native tissue units. The photomasks were placed on a cover slip between the UV light source and prepolymer solution to selectively expose the polymer to the light. A droplet containing 35μl of the photocrosslinkable PEG pre-polymer was placed on a glass slide covered by a cover slip separated by different numbers of spacers (cover slips, thickness = 150 μm) to provide hydrogel units with controlled thicknesses. UV light (360–480 nm; 12.4 mW/cm^2) was passed through the photomask for 27 seconds to polymerize the PEG in the desired microgel shapes. The entire self assembly procedure is illustrated in Figure 1.

Following UV polymerization, the building blocks were carefully detached from the OTS treated glass slide and randomly placed on the surface of dense, hydrophobic solutions (60ml) that were made of perfluorodecalin (PFDC) or carbon tetrachloride (CCl_4) (Aldrich)

NIH-PA Author Manuscript

NIH-PA Author Manuscript

NIH-PA Author Manuscript

in a standard 100 × 15mm Pyrex reusable Petri dish (Fisher Scientific). To quantify the degree of assembly the aggregation factor was calculated as defined above. To enhance the aggregation of microgels, stirring was applied to the system with different speeds using Corning stirrer (PC-620D, Preiser scientific). To create tissues from the aggregated, cell-laden microgels, following interface directed self assembly, the final product was exposed to UV for an additional 5s. Microgels were then washed 5× with PBS following PFDC exposure to remove excess PFDC and improve cell viability. In certain cases, to distinguish the microgels, the prepolymers were mixed with rhodamine-dextran (M_r= 10 kDa) or fluorescent FITC microbeads (1%, D= 5 μk; Duke Scentific) at a concentration of 0.3mM prior to the initial UV exposure.

Fabrication of Cell-Laden Microgel Assemblies

Fibroblast cells (NIH-3T3) were cultured in DMEM supplemented with 10% FBS (GIBCO) in a 5% CO_2 humidified incubator at 37°C. To harvest and encapsulate cells, the cells were first trypsinized with 1% trypsin (GIBCO) and centrifuged at 1000 RPM for 5 minutes. The harvested cells were mixed with PEG pre-polymer at a concentration of 1×10^7cells/ml. Cell-laden PEG was used in a similar manner to cell-free PEG to create microgels, as described above. To generate 3D model, co-cultures of different cell types, cells were separated into two groups and labeled with either Calcein AM (green) or PKH26 (red) fluorescent cell tracker (Sigma). In addition, co-cultured assemblies were performed in 5% w/v gelatin methacrylate (GelMA), instead of PEG, since GelMA has similar behavior to PEG, but allows cell elongation and migration.[29] To investigate cell viability at each stage, select unlabeled cell-laden microgels were analyzed using a live/dead assay according to the manufacturer's instructions (Molecular Probes).

Statistical Evaluation

Data were expressed as mean ± standard deviation (SD). Differences between groups were analyzed using student's one-tailed t-tests with p values less than 0.05 considered significant. Group size was n = 5 for all groups analyzed in parameter optimization part and was n=3 for cell viability test. $p < 0.05$ is represented by a single star and $p < 0.01$ is represented by a double star in the graphs. All error bars were presented as SD.

Acknowledgments

This paper was supported by the National Institutes of Health (EB007249; DE019024; HL092836), the NSF CAREER award, the Institute for Soldier Nanotechnology and the US Army Corps of Engineers. We would like to thank Drs. Yanan Du, Seunghwan Lee, Won Gu Lee and Jalil Mostashari for their scientific and technical support.

References

1. Langer R, Vacanti JP. Science 1993;260:920–926. [PubMed: 8493529]
2. Khademhosseini A, Vacanti JP, Langer R. Scientific American 2009;300:64–71. [PubMed: 19438051]
3. L'Heureux N, McAllister TN, de la Fuente LM. New Engl J Med 2007;357:1451–1453. [PubMed: 17914054]
4. Khademhosseini A, Langer R, Borenstein J, Vacanti JP. Proc Natl Acad Sci U S A 2006;103
5. Costanzo, L. Physiology. Saunders; Philadelphia: 2006.
6. Whitesides GM, Grzybowski B. Science 2002;295:2418–2421. [PubMed: 11923529]
7. Du Y, Lo E, Ali S, Khademhosseini A. Proc Natl Acad Sci U S A 2008;105:9522–9527. [PubMed: 18599452]
8. Dean DM, Napolitano AP, Youssef J, Morgan JR. FASEB 2007;21:4005–4012.

NIH-PA Author Manuscript

NIH-PA Author Manuscript

NIH-PA Author Manuscript

9. Napolitano AP, Chai P, Dean DM, Morgan JR. Tissue Eng 2007;13:2087–2094. [PubMed: 17518713]
10. Hoben GM, Hu JC, James RA, Athanasiou KA. Tissue Eng 2007;13:939–946. [PubMed: 17484700]
11. McGuigan AP, Sefton MV. Proc Natl Acad Sci U S A 2006;103:11461–11466. [PubMed: 16864785]
12. Peppas N, Hilt JZ, Khademhosseini A, Langer R. Adv Mater 2006;18:1–17.
13. Nicol JW, Khademhosseini A. Soft Matter 2009;5:1312–1319. [PubMed: 20179781]
14. Khademhosseini A, Langer R. Biomaterials 2007;28:5087–5092. [PubMed: 17707502]
15. Kralchevasky PA, Nagayama K. Adv Colloid Interf Sci 2000;85:145–192.
16. Bowden N, Terfort A, Carbeck J, Whitesides GM. Science 1997;276:233–235. [PubMed: 9092466]
17. Malchiodi-Albedi F, Perilli R, Formisano G, Scorcia G, Caiazza S. J Biomed Mater Res 1998;41:608–613. [PubMed: 9697034]
18. L'Heureux N, Dusserre N, Konig G, Victor B, Keire P, Wight TN, Chronos NA, Kyles AE, Gregory CR, Hoyt G, Robbins RC, McAllister TN. Nat Med 2006;12:361–365. [PubMed: 16491087]
19. McGuigan AP, Bruzewicz DA, Glavan A, Butte M, Whitesides GM. PLoS ONE 2008;3:1–11.
20. Allain C, Cloitre M. J Colloid Interf Sci 1993;157:261–268.
21. Grzybowski BA, Bowden N, Arias F, Yang H, Whitesides GM. J Phys Chem B 2001;105:404–412.
22. Mansfield EH, Sepangi HR, Eastwood EA. Philos Trans R Soc Lond A 1997:869–919.
23. Wolfe DB, Snead A, Mao C, Bowden NB, Whitesides GM. Langmuir 2003;19:2206–2214.
24. Whitesides GM, Boncheva M. Proc Natl Acad Sci USA 2002;99:4769–4774. [PubMed: 11959929]
25. Nguyen QH, Ponter AB, Peier W. J Chem Eng Data 2002;23:54.
26. Lam VT, Benson GC. Can J Chem 1970;48:3773–3781.
27. Dias AMA, Goncalves CMB, Caco AI, Santos L, Pineiro MM, Vega LF, Coutinho JAP, Marrucho IM. J Chem Eng Data 2005;50:1328–1333.
28. Freire MG, Carvalho PJ, Queimada AJ, Marrucho IM, Coutinho JAP. J Chem Eng Data 2006;51:1820–1824.
29. Benton JA, Deforest CA, Vivekanandan V, Anseth KS. Tissue Eng Pt A 2009;15:3221–3230.
30. Lamb, H. Statics, including hydrostatics and the elements of the theory of elasticity. Cambridge University Press; Cambridge, UK: 1912.
31. Fortes MA. Can J Chem 1982;60:2889–2895.
32. Shinto H, Komiyama D, Higashitani K. Langmuir 2006;22:2058–2064. [PubMed: 16489789]
33. Singh P, Joseph DD. J Fluid Mech 2005;530:31–80.
34. Nicolson MM. Proc Cambridge Philos Soc 1949;45:288–295.
35. Gifford WA, Scriven LE. Chem Eng Sci 1971;26:287–297.
36. Federovich NE, DeWijn JR, Verbout AJ, Alblas J, Dhert WJA. Tissue Eng Pt A 2008;14:127–133.
37. Roth EA, Xu T, Das M, Gregory C, Hickman JJ, Boland T. Biomaterials 2004;25:3707–3715. [PubMed: 15020146]
38. Mann BK, Gobin AS, Tsai AT, Schmedlen RH, West JL. Biomaterials 2001;22:3045–3051. [PubMed: 11575479]
39. Gobin AS, West JL. Faseb J 2002;16:751–753. [PubMed: 11923220]

NIH-PA Author Manuscript
NIH-PA Author Manuscript
NIH-PA Author Manuscript

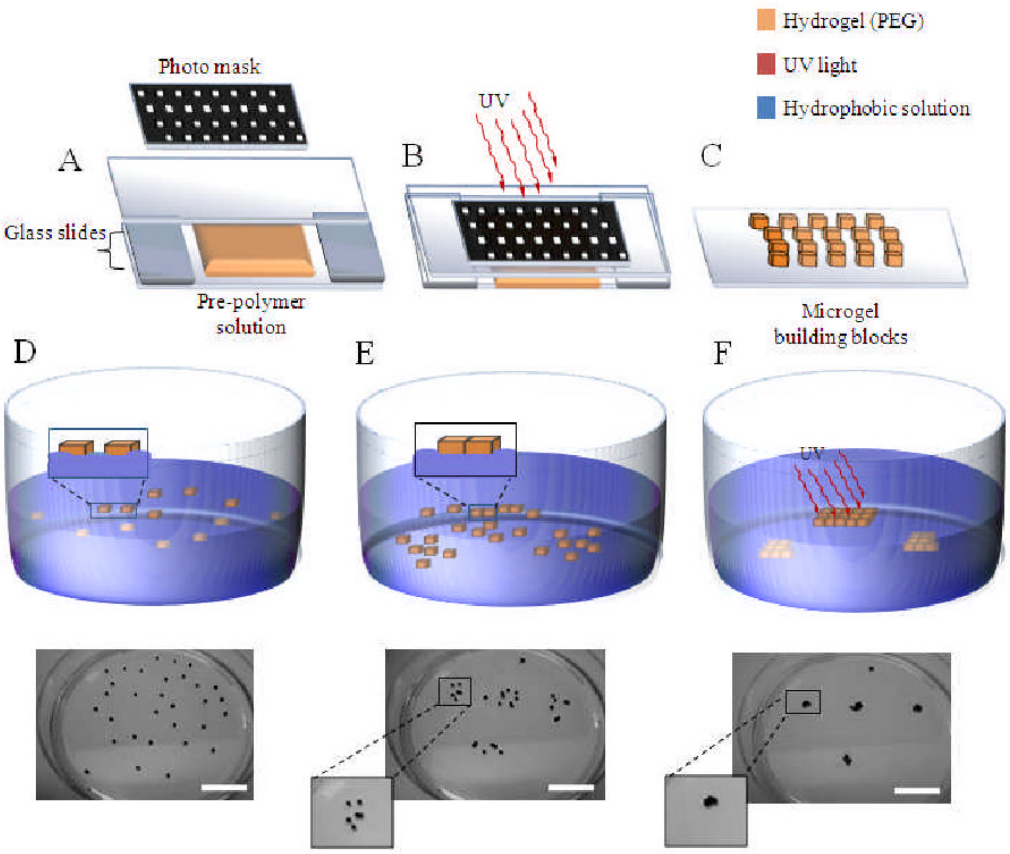

Figure 1.

Schematic illustration of the liquid-air interface directed self assembly technique. (A) PEG-cell solution was placed on top of an OTS-treated glass slide, between the photomask and spacers. (B) UV light was exposed through the photomask, causing the PEG-cell solution to polymerize in the desired pattern. (C) Following washing with PBS all that remained were cell-laden PEG microgels of the desired geometry. (D) Microgels were randomly placed on the surface of either PFDC or CCl_4 where they remained due to the high density of the solutions. (E) Due to surface tension, the particles self assembled to minimize free energy. (F) Secondary UV polymerization crosslinked the microgels to each other leading to macroscale engineered microgels. Scale bar: 2 cm

NIH-PA Author Manuscript
NIH-PA Author Manuscript
NIH-PA Author Manuscript

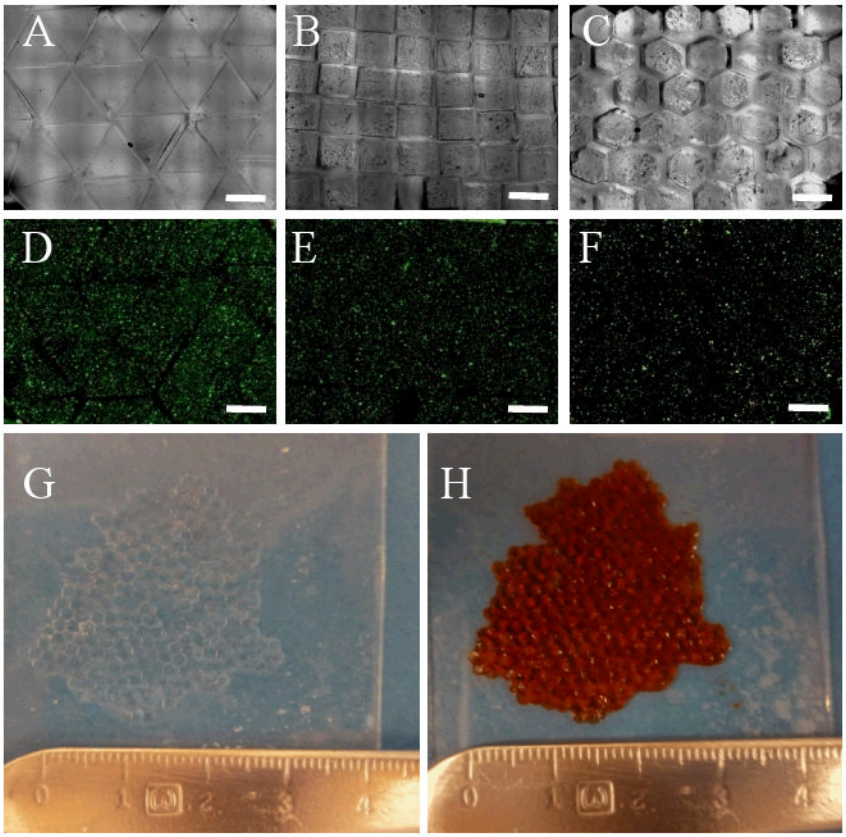

Figure 2.
Histological images of centimeter scale engineered gel sheets created by the interface directed assembly of microgel blocks. (A) Triangular, (B) square, and (C) hexagonal building blocks were assembled on the surface of either CCl_4 or PFDC and secondarily crosslinked to form engineered gel sheets. Live/dead staining demonstrated a high level of cell viability in all cases (D-F). (G) Formation of macroscale structures with overall dimensions on the centimeter scale made from hexagonal microgels, (H) to improve visualization the microgels were labeled with a red food coloring dye. Scale bar: 1 mm

NIH-PA Author Manuscript
NIH-PA Author Manuscript
NIH-PA Author Manuscript

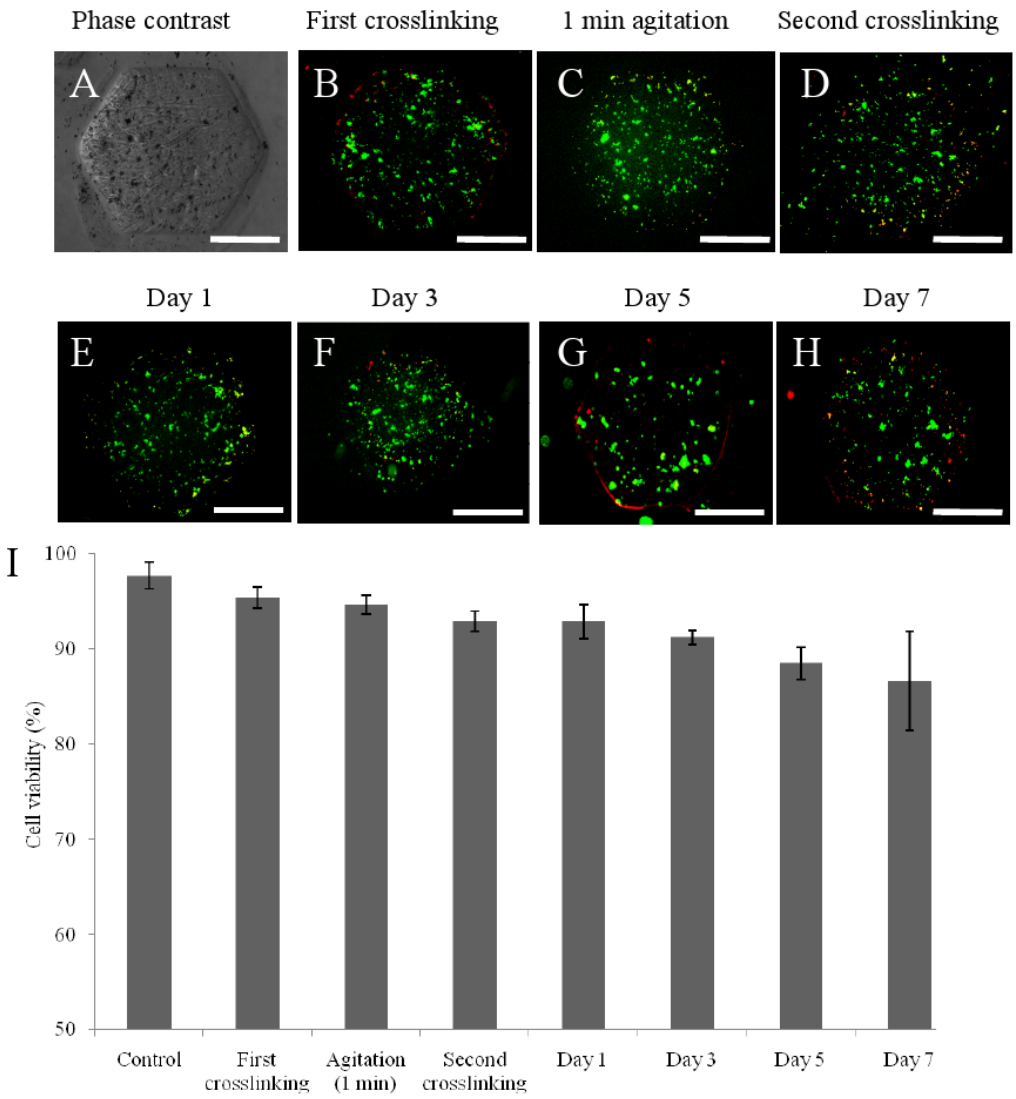

Figure 3.

Cell viability analysis as a function of steps in the assembly procedure. Hexagonal cell-laden hydrogels (A) were created and the viability was tracked following exposure to UV light and PFDC. PEG-cell mixtures were polymerized by UV exposure and placed on the surface of PFDC (B), stirred for 1 minute in PFDC (C) and secondarily crosslinked with UV light (D). Cell-laden microgels were then cultured for one (E), three (F), five (G) and seven (H) days in cell culture medium. Quantification of samples (n=5) at each timepoint (I) demonstrated that viability did not significantly decrease due to UV or PFDC exposure or time in culture. Scale bar: 500 μm

NIH-PA Author Manuscript

NIH-PA Author Manuscript

NIH-PA Author Manuscript

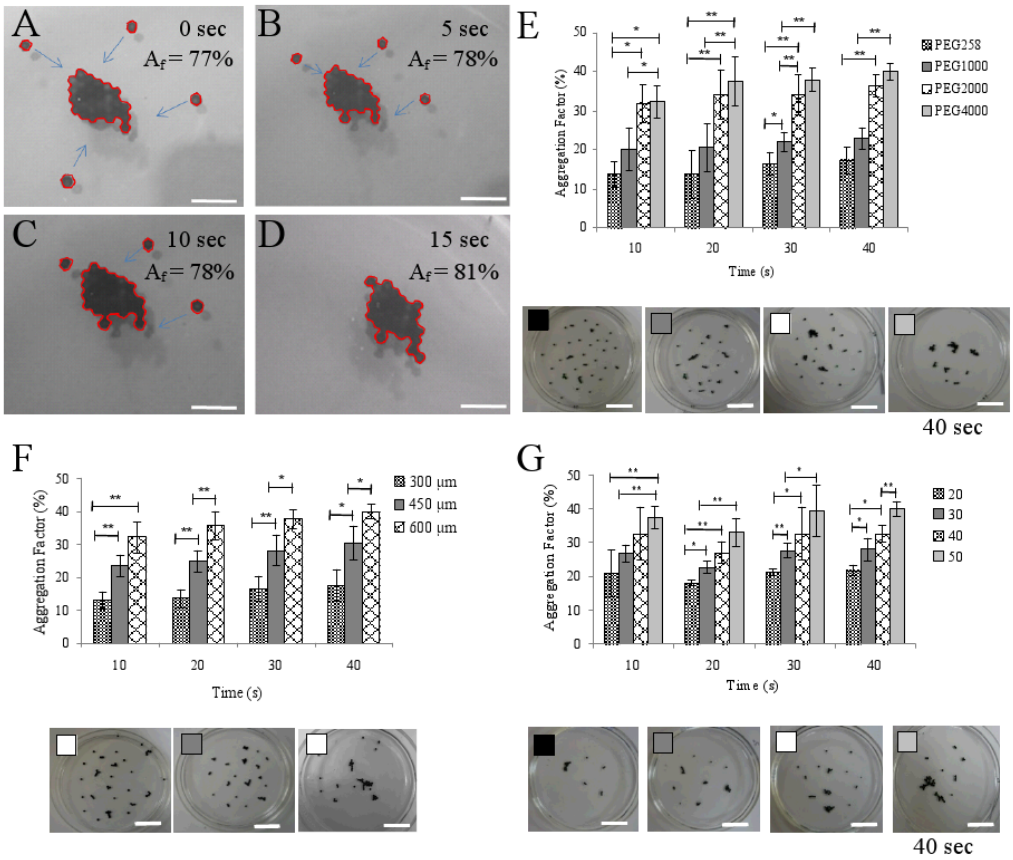

Figure 4.

Optimization of microgel assembly. (A-D) The assembly process was tracked in 5 second intervals to demonstrate how the aggregation factor (A_f) changed with time. (E) Increasing the molecular weight of PEG from 258 to 2000 significantly increased A_f. No further improvements were seen by using 4000 molecular weight PEG. (F) Increasing the thickness of the microgels from 300 μm to 450 μm ($p < 0.001$) and 450 μm to 600 μm ($p < 0.05$) significantly improved A_f. (G) Similarly, increasing the number of microgels on the solution surface significantly enhanced A_f ($p < 0.05$). Scale bar (A-D): 10 mm, Scale bar (E-G) : 2 cm

NIH-PA Author Manuscript
NIH-PA Author Manuscript
NIH-PA Author Manuscript

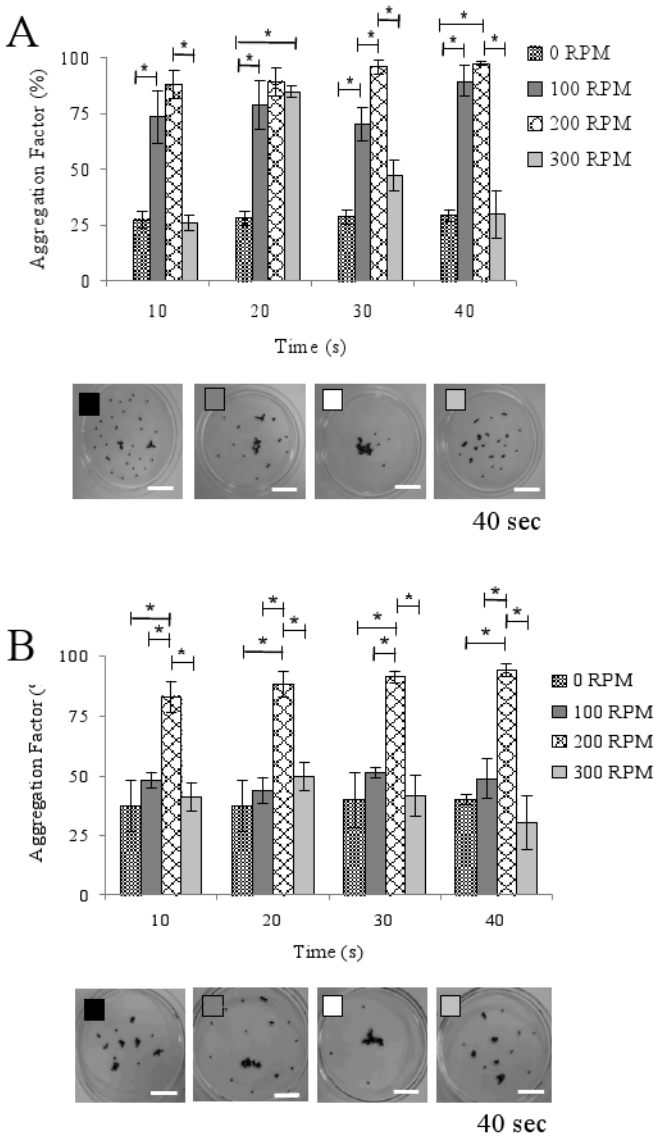

Figure 5.

Effects of stirring speed on interface directed microgel assembly. (A) Stirring at a speed of 100 RPM or 200 RPM caused a significantly higher A_f than no stirring ($p < 0.001$) or a stirring rate of 300 RPM ($p < 0.001$) on the surface of PFDC. (B) Generally similar behavior was seen for interface directed assembly on the surface of CCl_4, however, only a stirring speed of 200 RPM significantly improved A_f, while stirring rates of 100 or 300 RPM showed no improvement over static culture ($p < 0.001$). Inset: representative images of assembly following 40 sec agitation at each speed for PFDC and CCl_4. Scale bar: 2 cm

NIH-PA Author Manuscript
NIH-PA Author Manuscript
NIH-PA Author Manuscript

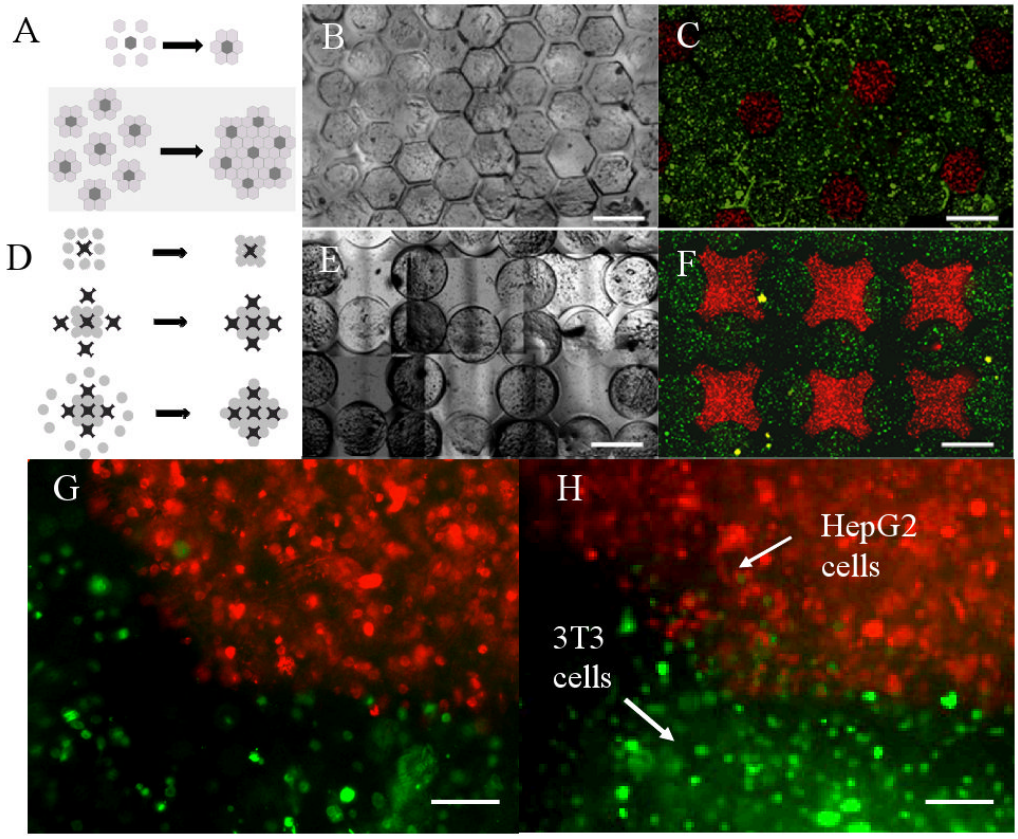

Figure 6.

Creation of interface directed microgel structures with controlled co-culture. (A) A cartoon representation of assembly of complex building blocks using a central microgel with 1 cell type (dark gray) surrounded by building blocks of a second cell type (light gray) on the surface of PFDC or CCl_4. The complex building blocks consisting of 7 hexagonal microgels could then be used for interface directed assembly into tissue-like structures with spatially controlled co-culture conditions. (B) Phase contrast and (C) fluorescent image of engineered centimeter-scale tissues using complex building blocks with controlled co-culture conditions. (D) A cartoon representation of assembly of complex building blocks with controlled co-culture using lock and key shaped microgels to better direct the assembly process. (E) Phase contrast and (F) fluorescent image of engineered centimeter-scale tissues using lock and key complex building blocks with controlled co-culture conditions. Scale bar: 1 mm. (G) The co-culture of 3T3 and HepG2 cells using the assembly process declared in (A), having blocks with encapsulated HepG2 cells surrounded with six blocks with encapsulated 3T3 cells after one day and (H) after seven days. Scale bar: 100μm